Proceedings of ICRC 2001: 2994 © Copernicus Gesellschaft 2001

ICRC 2001

Cosmic ray-induced high energy gamma-ray emission: a background for WIMP annihilation and massive relic particle models of UHE CR

T. A. Porter[1] **and R. J. Protheroe**[2]

[1]Defence Science and Technology Organisation, Sailsbury, SA, 5108, Australia
[2]Department of Physics and Mathematical Physics, University of Adelaide, SA 5001, Australia

Abstract. The possible discovery of a diffuse galactic halo in GeV gamma-rays has led to several possible dark matter explanations. An important consideration for these models is the uncertainty in the galactic diffuse gamma-ray background. For example, the predicted inverse Compton signal can vary significantly depending on the choice of cosmic ray halo size, or even on the electron injection spectral index. Using a self-consistent propagation model we calculate the distribution of galactic cosmic ray electrons and positrons. Diffuse gamma-ray spectra are obtained using the results of the propagation calculations. We show our results for different propagation model parameters and electron injection spectral indices.

1 Introduction

The possible observation of a diffuse galactic halo in GeV gamma-rays by Dixon et al. (1998) (see also Chary & Wright 1998) has led to several possible dark matter explanations. For example, Gondolo (1999) suggests that this may be due to annihilation of relic WIMPs with mass $\sim 2-4$ GeV corresponding to a relic density $\Omega \sim 0.1$. Fargion (2000) suggests that it could be due to annihilation of heavy relic neutrinos, N, with mass in the range $m_Z/2$ to m_Z followed by inverse Compton (IC) scattering of electron pairs or decay of π^0 mesons produced as a result of $N \rightarrow q\overline{q}$. They conclude that the predicted halo flux is consistent with that observed. De Paolis et al. (1999) suggest that cold H_2 clouds may be clumped in dark clusters (possibly MACHOs) in the galactic halo. Cosmic ray interactions would then produce a γ-ray intensity at GeV energies which would be anisotropic. For all of these possibilities there would be an important background due to inverse Compton (IC) scattering of cosmic ray electrons and positrons on the galactic radiation fields and cosmic microwave background. However, the contribution by such an IC component is uncertain, depending on the scale-height of the electron/positron distribution, scale-height of the radiation field distribution, and even on the injection spectrum of primary cosmic ray electrons at acceleration (e.g. Porter & Protheroe 1997). Hence, to disentangle any dark matter initiated gamma-ray signal it is necessary to ascertain what variations in the galactic diffuse component, particularly those due to IC interactions, are possible.

In this paper, we address the question of what are the significant parameters influencing predictions of the galactic diffuse gamma-ray component, and what variations in the calculated diffuse spectrum can result from variations of these parameters within allowed limits. Using a self-consistent propagation model we calculate the distribution of electrons and positrons in the Galaxy. We determine the upper and lower limits on the propagation model parameters from cosmic ray radio-isotope data and use these as input to our propagation calculations. We use the calculated electron and positron distributions to obtain diffuse photon emissivity spectra as a function of position in the Galaxy. Diffuse photon intensity spectra are obtained from line-of-sight calculations using the predicted emissivity spectra. We then compare our model predictions with available satellite data, and with dark matter predictions by other authors.

2 Propagation Calculations

We use a Monte Carlo code for propagating electrons and positrons in the Galaxy (Porter 1999), and we assume the Galaxy has a cylindrical geometry with a maximum radial dimension of $R_{\rm max} = 20$ kpc. The propagation calculations are performed using a three-dimensional (3D) diffusion model, but the electron and positron distributions are obtained only for the 2D case (R, z) to take into account the 2D nature of the models for the matter distribution, radiation field and magnetic field we use.

In our adopted propagation model the free parameters are the halo size, z_h, beyond which cosmic rays escape the Galaxy, and the diffusion coefficient at low energy, K_0. To fix these

Correspondence to: tporter@physics.adelaide.edu.au

parameters we performed a propagation model analysis (Porter 1999) of the abundances of ^{10}Be and ^{26}Al measured by the Voyager spacecraft (Lukasiak et al. 1994a,b). From this analysis we obtained z_h values between 3 kpc and 5 kpc. The corresponding K_0 values were 3.2×10^{28} cm^2 s^{-1} and 5.3×10^{28} cm^2 s^{-1} respectively. These limits correspond to the lower and upper limits on the halo size consistent with both sets of cosmic ray radio-isotope data. For our propagation model the rigidity dependence of the diffusion coefficient was assumed to be constant below a rigidity of $\rho = 4.7$ GV and to increase as $K_0(\rho/4.7\ \mathrm{GV})^{0.6}$ above 4.7 GV (Webber et al. 1996).

For the spatial source distribution of primary electron sources we adopt the radial distribution given by Strong & Moskalenko (1998) and assume a uniform z distribution with half-height $z_d = 0.2$ kpc. The injection spectrum of primary electrons is taken as a power-law, $Q(E) \propto E^{-\gamma}$, and we consider values of γ at injection in the range $1.8 - 2.4$. We take the galactocentric radius of the Sun to be $R_S = 8.5$ kpc. Secondary electrons and positrons are assumed to be produced in inelastic collisions between cosmic ray nuclei and gas in the interstellar medium, and the source function for these particles is constructed as described by Porter (1999).

We use realistic models of the radiation fields (Porter 1999), matter distribution (Dickey and Lockman 1990; Bronfman et al. 1988; Cordes et al. 1991), and magnetic field (Beck et al. 1996). Electrons lose energy while propagating via ionisation, bremsstrahlung, synchrotron and IC processes; for IC losses we include Klein-Nishina effects at high energies.

Figure 1 shows a comparison of direct measurements of the electron intensity spectrum in the solar vicinity, spectra derived from non-thermal radio measurements and our calculated spectra using the Monte Carlo method for injection indices $\gamma = 1.8$ and $\gamma = 2.4$ with $z_h = 5$ kpc (the $z_h = 3$ kpc local spectra do not appreciably differ). The normalisation for the primary spectra are obtained by adjusting the predicted primary spectra so that the total spectra (primary + secondary) agree with the observations around 10 GeV (Nishimura et al. 1995 and references therein). At high energies both of the calculated spectra over-predict the data to some degree. However, because of the strong energy losses by electrons, the spectrum of directly observed primary electrons will be sensitive to the distance to the nearest electron source, whereas the spectrum averaged over a larger volume may be significantly higher. Therefore, we do not require agreement between our calculated spectra and that locally observed above 30 GeV or so (Pohl & Esposito 1998; Porter 1999 and references therein).

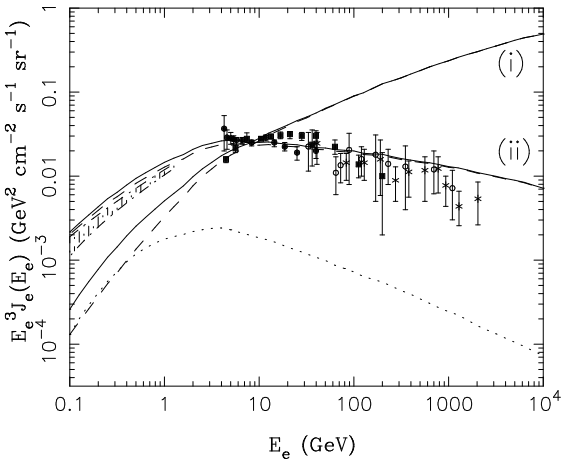

Fig. 1. Local interstellar electron spectrum (primary electrons + secondary electrons and positrons) calculated with $z_h = 5$ kpc for injection spectral indices (i) $\gamma = 1.8$ and (ii) $\gamma = 2.4$. Solid line: total spectra; dashed line: primary electron spectra; dotted line: secondary electron and positron spectrum. Data: Nishimura et al. (1995) and references therein. Note that the secondary electron spectum is independent of the injection spectrum of primary electrons, depending instead mainly on the the observed spectrum of cosmic ray protons and nuclei, and is rather insensitive to halo sizes in the range adopted here.

3 Diffuse Photon Spectra

Using our predicted electron and positron distributions, we calculate the diffuse photon emissivity due to synchrotron, bremsstrahlung and IC interactions, and perform line-of-sight integrations to obtain the intensity spectra of diffuse galactic radiation. We calculate the emissivity of π^0-decay photons using the same hadronic interaction model, cosmic ray and gas distributions as for the secondary electron/positron source distribution. We use the observed galactic non-thermal emission to select plausible values for the primary injection spectrum corresponding to the upper and lower limits on the

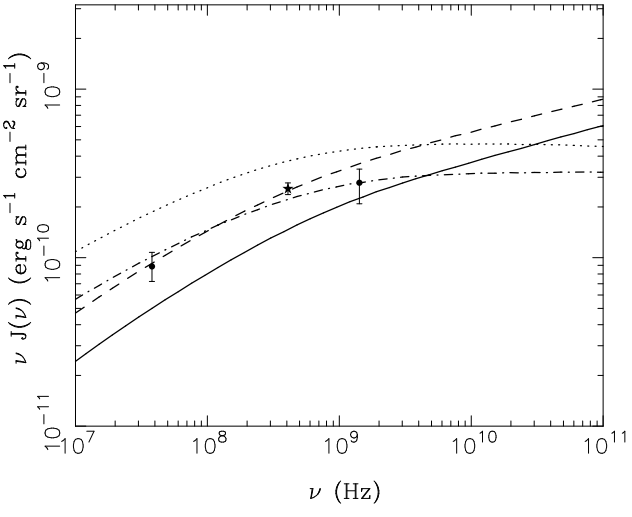

Fig. 2. Non-thermal intensity in the direction of the galactic pole. Solid line: $\gamma = 1.8$ and $z_h = 3.0$ kpc; Dashed line: $\gamma = 1.8$ and $z_h = 5.0$ kpc; Dot-dashed line: $\gamma = 2.2$ and $z_h = 3.0$ kpc; dotted line: $\gamma = 2.2$ and $z_h = 5.0$ kpc. Data: Lawson et al. (1987) (38 MHz), Broadbent et al. (1990) (408 MHz) and Reich & Reich (1988) (1420 MHz).

halo size used in the propagation calculations. Figure 2 compares our predicted non-thermal spectra with high latitude data (Lawson et al. 1987; Reich & Reich 1988; Broadbent et al. 1989) for $z_h = 3$ kpc and $z_h = 5$, and $\gamma = 1.8$ and $\gamma = 2.2$. For a halo size $z_h = 3.0$ kpc the injection spectrum most compatible with the data is $\gamma \sim 2.2$. For $z_h = 5.0$ kpc the injection spectrum agreeing best with the data is $\gamma \sim 1.8$.

Using these z_h/γ combinations, we calculate the diffuse gamma-ray spectrum at high latitudes and compare with observations. Figure 3 compares our predictions with available satellite data on the total (extragalactic + galactic) spectrum (Kinzer et al. 1997; Strong, Moskalenko & Reimer 1998 and references therein) for $z_h = 5.0$ kpc and $\gamma = 1.8$ (3a - model-I), and $z_h = 3.0$ kpc and $\gamma = 2.2$ (3b - model-II). In the figures our predicted spectra include emission by synchrotron radiation, bremsstrahlung, IC and π^0-decay. The unusual spectrum below 1 MeV is a result of including the contribution by synchrotron emission for different high energy cut-offs in the electron injection spectrum (Porter & Protheroe 1997, 1999), which we expect to occur at high energies (Protheroe & Stanev 1999). Since the synchrotron emission is used to constrain the injection spectrum, self-consistency requires that the emission at higher energies by this process also be included in the models.

Below a few MeV the model predictions account for, at most, only a few percent of the total spectrum, which is presumably due to Seyfert I and II galaxies and a contribution by supernovae (Zdziarski 1996). At higher energies the predicted spectra comprise a significantly greater fraction of the total spectrum, which at these energies may be due in part to unresolved blazars (Sreekumar et al. 1998 and references therein). For energies greater than a few tens of MeV up to about 1 GeV our models predict approximately 50% of the total flux can be due to galactic processes. For higher energies than ~ 1 GeV variations in the contribution to the total flux due to different injection spectral indices and halo sizes are much more noticeable. For our model-I a very large fraction ($\sim 80 - 85\%$) of the high latitude flux can be due to galactic processes, the majority of which ($\sim 55\%$) comes from IC interactions and π^0-decay ($\sim 40\%$). For our model-II about $50-55\%$ can be due to galactic processes with about $25-30\%$ coming from IC interactions and $\sim 10-20\%$ from bremsstrahlung, the rest being due to π^0-decay.

4 Discussion

We discuss our model calculations and compare our results with other calculations on the contributions by various dark matter hypotheses to the diffuse gamma-ray flux. Our models show that a significant fraction of the total flux can be due to galactic processes. For the model giving the greatest contribution (model-I - $\gamma = 1.8$, $z_h = 5.0$ kpc) we obtain an integrated flux above 100 MeV of 1.1×10^{-5} cm^{-2} s^{-1} sr^{-1}, while for the other model (model-II) we obtain an integrated flux above 100 MeV of 8.8×10^{-6} cm^{-2} s^{-1} sr^{-1}. These results can be compared with the measured value above 100 MeV by EGRET of $1.45 \pm 0.05 \times 10^{-5}$ cm^{-2} s^{-1} sr^{-1} (Sreekumar et al. 1998). Therefore, it is possible that $60 - 80\%$ of the measured flux above 100 MeV can be attributed to galactic processes alone. We note that above 1 GeV our models give integrated fluxes of 1.4×10^{-6} cm^{-2} s^{-1} sr^{-1} (model-I) and 8.5×10^{-7} cm^{-2} s^{-1} sr^{-1} (model-II) respectively.

Various calculations of the contribution to the diffuse gamma-ray background by different dark matter hypotheses have been made. For baryonic dark matter models, De Paolis et al. (1999) calculate an integrated flux above 100 MeV of $\sim 5.9 \times 10^{-6}$ cm^{-2} s^{-1} sr^{-1}, and an integrated flux above 1 GeV of $\sim 6-8 \times 10^{-7}$ cm^{-2} s^{-1} sr^{-1}. For gamma-rays from superheavy relic particles, Blasi (1999) obtains an integrated flux above 100 MeV of $\sim 10^{-8}$ cm^{-2} s^{-1} sr^{-1} for his best case scenario. For relic WIMP annihilations Gondolo (1999) obtains a flux above 100 MeV of $\sim 1-2 \times 10^{-8}$ cm^{-2} s^{-1} sr^{-1} for masses in the range $2 - 4$ GeV. Only one of these calculations (De Paolis et al. 1999) gives a flux comparable to our results. All others are significantly lower than the possible variation in the galactic component we calculate.

To summarise, we have used a propagation model to calculate the distribution of electrons and positrons in the Galaxy for two halo sizes that represent the upper and lower limits allowed by an analysis of cosmic ray radio-isotope data. The galactic non-thermal emission has then been used to determine the most likely values for the electron injection spectral index that correspond to the upper and lower limit halo sizes used in the propagation calculations. For these models, we have calculated the diffuse gamma-ray spectrum and compared our results with published values for the diffuse gamma-ray spectrum. We have compared the results of our calculations with calculations made of the contribution by various dark matter hypotheses to the diffuse galactic emission. We find that the contribution to the total measured flux by the galactic component in our models can be between $50 - 85\%$ depending on the choice of halo size and electron injection spectrum. This variation in the possible galactic component is significant and shows that providing tighter constraints on the parameters influencing predictions of the galactic contribution to the diffuse gamma-ray spectrum are crucial for disentangling signals such as might come from dark matter scenarios of gamma-ray production.

References

Beck, R. et al., Galactic Magnetism: Recent Developments and Perspectives, Ann. Rev. Astron. Astrophys., **34**, 155-206, 1996.

Blasi, P., Gamma rays from superheavy relic particles in the halo, Phys. Rev. D, **60**, 23514, 1999.

Broadbent, A. et al., A technique for separating the galactic thermal radio emission from the non-thermal component by means of the associated infrared emission, Mon. Not. R. Astron. Soc., **237**, 381-410., 1989.

Bronfman, L. et al., A CO survey of the southern Milky Way - The mean radial distribution of molecular clouds within the solar circle, Astrophys. J., **324**, 248-266, 1988.

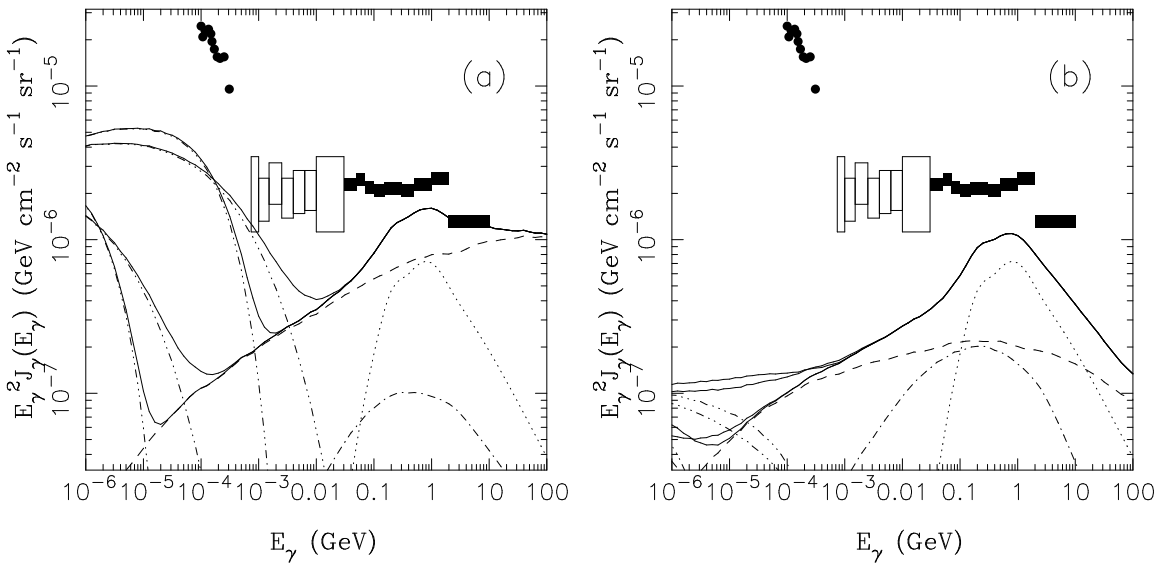

Fig. 3. Diffuse high latitude intensity spectra $(-180^\circ \leq l \leq 180^\circ, |b| > 70^\circ)$ for injection spectrum (a) $\propto E^{-1.8}$ and $z_h = 5.0$ kpc, (b) $\propto E^{-2.2}$ and $z_h = 3.0$ kpc. Theoretical predictions: IC (dashed line); π^0-decay (dotted line); dash-dotted line (bremsstrahlung); synchrotron for a high energy cut-off in the injection spectrum of 100 TeV and 1000 TeV (triple dot-dashed lines, the two curves for each case being for a sharp and an exponential cut-off); total spectrum (solid lines). Data (total intensity spectra for high latitudes): HEAO-1 (closed circles); COMPTEL (open boxes); EGRET (solid boxes).

Chary, R. and Wright, E. L., The High Energy Gamma-Ray Background as a Probe of the Dark Matter in the Galactic Halo, in *The Third Stromlo Symposium: The Galactic Halo* eds. Gibson, B. K., Axelrod, T. S. & Putman, M. E., ASP Conference Series, **165**, 357-361, 1998.

Cordes, J. M. et al., The Galactic distribution of free electrons, Nature, **354**, 121-124, 1991.

De Paolis, F. et al., Gamma-Ray Astronomy and Baryonic Dark Matter, Astrophys. J., **510**, L103-L106, 1999.

Dickey, J. M. and Lockman, P. J., H I in the Galaxy, Ann. Rev. Astron. Astrophys., **28**, 215-261, 1990.

Dixon, D. D., et al., Evidence for a Galactic gamma-ray halo, New Astron., **3**, 359-561, 1998.

Fargion, D., Galactic gamma halo by heavy neutrino annihilations? , Astropart. Phys., **12**, 307-314, 2000.

Gondolo, P., WIMP annihilations and the galactic gamma-ray halo, in *Dark matter in astrophysics and particle physics, 20-25 July 1998, Heidelberg, Germany* eds. Klapdor-Kleingrothaus, H. V. & Baudis, L., Institute of Physics Publishing, Philadelphia, PA, p.531, 1999.

Kinzer, R. L. et al., Diffuse Cosmic Gamma Radiation Measured by HEAO 1, Astrophys. J., 475, 361-372, 1997.

Lawson, K. D. et al., Variations in the Spectral Index of the Galactic Radio Continuum Emission in the Northern Hemisphere, Mon. Not. R. Astron. Soc., **225**, 307-327, 1987.

Lukasiak, A., Ferrando, P., McDonald, F. B. and Webber, W. R., The isotopic composition of cosmic-ray beryllium and its implication for the cosmic ray's age, Astrophys. J., **423**, 426-431, 1994a.

Lukasiak, A., Ferrando, P. and Webber, W. R., Voyager measurements of the isotopic composition of cosmic-ray aluminum and implications for the propagation of cosmic rays, Astrophys. J., **430**, 69L-L72, 1994b.

Nishimura, J. et al., Astrophysical significance of the confinement time of primary electrons in the galaxy, *Proc. 24th ICRC, Rome*, **3**, 29-32, 1995.

Pohl, M. and Esposito, J. A., Electron Acceleration in Supernova Remnants and Diffuse Gamma Rays above 1 GeV, Astrophys. J., **507**, 327-338, 1998.

Porter, T. A. and Protheroe, R. J., Cosmic-ray electrons and the diffuse gamma-ray spectrum, J. Phys. G: Nucl. Part. Phys., **23**, 1765-1784, 1997.

Porter, T. A., Ph.D. Thesis *Signatures of the Propagation of Cosmic Ray Electrons and Positrons in the Galaxy*, University of Adelaide, 1999.

Porter, T. A. and Protheroe, R. J., Constraints on the electron injection spectrum from diffuse gamma-ray observations *Proc. 26th ICRC, Salt Lake City*, 4, 306-309, 1999.

Protheroe, R. J. and Stanev, Todor, Cut-offs and pile-ups in shock acceleration spectra, Astropart. Phys., **10**, 185-196, 1999.

Reich, P. and Reich, W., Spectral index variations of the Galactic radio continuum emission - Evidence for a Galactic wind, Astron. & Astrophys., **196**, 211-226, 1988.

Sreekumar, P. et al., EGRET Observations of the Extragalactic Gamma-Ray Emission, Astrophys. J., **494**, 523-534, 1998.

Strong, A. W. and Moskalenko, I. V., Propagation of Cosmic-Ray Nucleons in the Galaxy, Astrophys. J., **509**, 212-228, 1998.

Strong, A. W., Moskalenko, I. V. and Reimer, O., Diffuse Continuum Gamma Rays from the Galaxy, Astrophys. J., **537**, 763-784, 2000.

Webber, W. R., Lukasiak, A., McDonald, F. B. and Ferrando, P., New High-Statistical–High-Resolution Measurements of the Cosmic-Ray CNO Isotopes from a 17 Year Study Using the Voyager 1 and 2 Spacecraft, Astrophys. J., **457**, 435-439, 1996.

Zdziarski, A. A., Contributions of AGNs and SNe IA to the cosmic X-ray and gamma-ray backgrounds, Mon. Not. R. Astron. Soc., **281**, L9-L13, 1996.